

were recorded for the same pulse duration  $\theta$ (s), by varying the anodic step potential by 10-mV increments starting from the potential corresponding to  $E^p + 100$  mV where  $E^p$  was the peak potential of wave  $O_2$  (correspondingly  $O_3$ ) at a scan rate  $v$ (V·s<sup>-1</sup>) = 1/(40 $\theta$ ).<sup>31b</sup> The values of  $R_{O_2}$  (correspondingly  $R_{O_3}$ ) shown in Figures 4 and 6 were selected so that, after correction from the background current, they were independent of the step potential.<sup>41</sup>

**General Procedure for Preparative Scale Electrochemistry.** THF (40 mL) and *n*-Bu<sub>4</sub>NBF<sub>4</sub> (2.7 g) were introduced in each compartment of the cell under argon atmosphere. To be consistent with the results of transient electrochemistry, electrolyses were done on solutions 2 mM in Pd<sup>II</sup>Cl<sub>2</sub>(PPh<sub>3</sub>)<sub>2</sub>. Thus 0.08 mmol (56 mg) of Pd<sup>II</sup>Cl<sub>2</sub>(PPh<sub>3</sub>)<sub>2</sub> and 1,2-dichloroethylene (10 equiv) were introduced in the cathodic compartment. Electrolysis was then performed at -1.4 V vs SCE and was interrupted after the current dropped to ca. 5% of its initial value. Charge integration showed that this corresponded to ca. 2 faradays per mol of Pd<sup>II</sup>Cl<sub>2</sub>(PPh<sub>3</sub>)<sub>2</sub>. For <sup>31</sup>P NMR studies, an NMR tube filled with argon and equipped with a septum was filled with this solution using a cannula according to standard Schlenk procedures.

**Product Identification.** For the (*Z*)- or the (*E*)-1,2-dichloroethylene, the reaction products observed within the time scale of transient electrochemistry were too unstable to be isolated and characterized (except by their <sup>31</sup>P NMR). In each case they rearranged to their thermody-

namically more stable trans isomer<sup>4b,8</sup> which was isolated as the final product of the reaction. For example, after electrolysis, in the case of the (*E*)-1,2-dichloroethylene, the <sup>31</sup>P NMR spectrum consisted of a broad signal ( $\Delta$  420 Hz) at 19.77 ppm and of a sharp peak at 23.91 ppm. The peak at 19.77 ppm totally disappeared within 2.5 h while the peak at 23.91 increased concomitantly. This latter was identical with that obtained (23.73 ppm) for an authentic sample of the corresponding *trans*- $\sigma$ -(*E*)-vinylpalladium complex.<sup>8a</sup>

**Reaction of Trichloroethylene with Pd<sup>0</sup>(PPh<sub>3</sub>)<sub>4</sub>.** Trichloroethylene and Pd<sup>0</sup>(PPh<sub>3</sub>)<sub>4</sub> were reacted according to a published procedure.<sup>8a</sup> However, in contradiction with ref 8a, which reports only one product, i.e. *trans*-[Cl<sub>2</sub>C=CHPd<sup>II</sup>(PPh<sub>3</sub>)<sub>2</sub>Cl], after workup <sup>1</sup>H NMR (250 MHz in CDCl<sub>3</sub> relative to TMS) showed the presence of two major constituents: *trans*-[Cl<sub>2</sub>C=CHPd<sup>II</sup>(PPh<sub>3</sub>)<sub>2</sub>Cl] (80%; 5.10 ppm, t,  $J_{HP}$  = 0.75 Hz) and (*Z*)-*trans*-[ClCH=CClPd<sup>II</sup>(PPh<sub>3</sub>)<sub>2</sub>Cl] (20%; 5.95 ppm, t,  $J_{HP}$  = 6 Hz), with a poorly resolved signal at 5.28 ppm tentatively attributable to traces of the third isomer, i.e. (*E*)-*trans*-[ClCH=CClPd<sup>II</sup>(PPh<sub>3</sub>)<sub>2</sub>Cl].

**Acknowledgment.** This work has been supported in part by the Centre National de la Recherche Scientifique (CNRS, URA 1110 "Activation Moléculaire") and Ecole Normale Supérieure. We are greatly indebted to Dr. Gérard Linstrumelle for calling our attention to the subject of this study and for invaluable stimulating discussions in the early stages of this project. Drs. Merete Nielsen and Walter Bowyer are gratefully acknowledged for their constructive readings of this manuscript.

(41) Amatore, C.; Lexa, D.; Savéant, J. M. *J. Electroanal. Chem.* **1980**, *111*, 81.

## Characterization of Transition States by Isotopic Mapping and Structure-Reactivity Coefficients: Solvent and Secondary Deuterium Isotope Effects for the Base-Catalyzed Breakdown of Acetaldehyde Hemiacetals

Charolotte A. Coleman and Christopher J. Murray\*

Contribution from the Department of Chemistry and Biochemistry, University of Arkansas, Fayetteville, Arkansas 72701. Received May 7, 1990

**Abstract:** Rate constants and structure-reactivity coefficients for the breakdown of acetaldehyde and acetaldehyde-*d*<sub>4</sub> hemiacetals were determined in water and deuterium oxide by trapping the acetaldehyde formed with  $\alpha$ -effect nucleophiles. General-base catalysis by substituted acetate and cacodylate ion catalysts represents equilibrium ionization of the hemiacetal CL<sub>3</sub>CL(OL)OR (L = H or D) to form the hemiacetal anion, CL<sub>3</sub>CL(O<sup>-</sup>)OR followed by rate-determining general-acid catalysis of the cleavage of the hemiacetal anion to form acetaldehyde and ROL. Solvent isotope effects for the catalytically active proton  $k_p^{BH}/k_p^{BD}$  = 0.9–2.5 do not change significantly with changes in the pK of the catalyst or the leaving group alcohol. The increase in the secondary  $\alpha, \beta$ -deuterium isotope effects  $k^{\alpha\beta H}/k^{\alpha\beta D}$  = 1.21–1.30 with decreases in the pK of the leaving group alcohol can be described by the interaction coefficient  $p_{xy} = \partial p_n / -\partial pK_{lg} = -0.069$ . The increase in Brønsted  $\beta$  = 0.48–0.72 with decreases in the pK of the leaving group alcohol in water can be described by the interaction coefficient  $p_{xy} = \partial \beta / -\partial pK_{lg} = 0.090$  and in D<sub>2</sub>O by  $p_{xy} = 0.078$ . The interaction coefficients and the observation of *both* solvent and secondary deuterium isotope effects are consistent with a coupling between proton transfer to the leaving group oxygen and changes in hybridization about the central carbon in the transition state for cleavage of the hemiacetal anion. The results are discussed in the context of proposals for stable hydrogen-bonded protons in concerted acid- and base-catalyzed reactions in water.

### Introduction

Reaction progress or bond order in the transition state is usually estimated from kinetic isotope effects or observed structure-reactivity coefficients.<sup>1,2</sup> For example, an empirical approach is

based on changes in Brønsted coefficients with changes in structure that can be described by interaction coefficients. The relative contributions of bond-making and bond-breaking processes in the transition state can be calculated from these interaction coefficients.<sup>3</sup> This approach has been used to characterize the mechanisms of the addition of nucleophiles to electrophilic carbonyl compounds as illustrated in eq 1 for the formation of hemiacetal anions.

An alternative strategy is to substitute heavy isotopes for the atoms undergoing changes in bonding. In that case, the magnitude of the kinetic isotope effect reflects the differences in vibrational

(1) For reviews see: (a) Bell, R. P. *The Proton in Chemistry*, 1st ed.; Cornell University Press: Ithaca, NY, 1959 (2nd ed.; Chapman and Hall: London, 1973). (b) Cleland, W. W., O'Leary, M. H., Northrop, D. B., Eds. *Isotope Effects on Enzyme-Catalyzed Reactions*; University Park Press: Baltimore, MD, 1977. (c) Gandour, R. D., Schowen, R. L., Eds. *Transition States of Biochemical Processes*; Plenum Press: New York, 1978. (d) Melander, L.; Saunders, W. H., Jr. *Reaction Rates of Isotopic Molecules*; Wiley: New York, 1980.

(2) Jencks, W. P. *Chem. Rev.* **1985**, *85*, 511.

(3) Jencks, D. A.; Jencks, W. P. *J. Am. Chem. Soc.* **1977**, *99*, 7948.



**Table I.** Rate Constants for General-Base-Catalyzed Breakdown of Acetaldehyde Hemiacetals CH<sub>3</sub>CH(OL)OR in Water and Deuterium Oxide

catalyst	pK <sub>a</sub> <sup>BL</sup>		k <sub>B</sub> , M <sup>-1</sup> s <sup>-1</sup>		k <sub>B</sub> <sup>H</sup> /k <sub>B</sub> <sup>D</sup>	k <sub>p</sub> <sup>BL</sup> /k <sub>p</sub> <sup>BD</sup> <sup>a</sup>
	H <sub>2</sub> O	D <sub>2</sub> O	H <sub>2</sub> O	D <sub>2</sub> O		
			ROH = CH <sub>3</sub> CH <sub>2</sub> OH (pK <sub>a</sub> = 16; <sup>b</sup> β = 0.48) <sup>c</sup>			
CH <sub>3</sub> OCH <sub>2</sub> COO <sup>-</sup>	3.40	3.87	6.2 × 10 <sup>-3</sup>	5.3 × 10 <sup>-3</sup>	1.2	0.8
ClCH <sub>2</sub> CH <sub>2</sub> COO <sup>-</sup>	3.93	4.40	1.36 × 10 <sup>-2</sup>	6.35 × 10 <sup>-3</sup>	2.14	1.4
CH <sub>3</sub> COO <sup>-</sup>	4.65	5.17	2.17 × 10 <sup>-2</sup>	7.89 × 10 <sup>-3</sup>	2.75	2.0
(CH <sub>3</sub> ) <sub>2</sub> AsO <sub>2</sub> <sup>-</sup>	6.16	6.68	1.45 × 10 <sup>-1</sup>	6.31 × 10 <sup>-2</sup>	2.30	1.6
			ROH = ClCH <sub>2</sub> CH <sub>2</sub> OH (pK <sub>a</sub> = 14.31; <sup>b</sup> β = 0.57) <sup>c</sup>			
ClCH <sub>2</sub> COO <sup>-</sup>	2.70		2 × 10 <sup>-3</sup>			
CH <sub>3</sub> OCH <sub>2</sub> COO <sup>-</sup>	3.40	3.87	5.7 × 10 <sup>-3</sup>	3.3 × 10 <sup>-3</sup>	1.7	1.1
ClCH <sub>2</sub> CH <sub>2</sub> COO <sup>-</sup>	3.93	4.40	1.09 × 10 <sup>-2</sup>	5.96 × 10 <sup>-3</sup>	1.83	1.2
CH <sub>3</sub> COO <sup>-</sup>	4.65	5.17	2.05 × 10 <sup>-2</sup>	1.00 × 10 <sup>-2</sup>	2.05	1.5
(CH <sub>3</sub> ) <sub>2</sub> AsO <sub>2</sub> <sup>-</sup>	6.16	6.68	2.15 × 10 <sup>-1</sup>	1.02 × 10 <sup>-1</sup>	2.11	1.5
			ROH = HC≡CCH <sub>2</sub> OH (pK <sub>a</sub> = 13.55; <sup>b</sup> β = 0.72) <sup>c</sup>			
CH <sub>3</sub> OCH <sub>2</sub> COO <sup>-</sup>	3.40	3.87	6.6 × 10 <sup>-3</sup>	5.0 × 10 <sup>-3</sup>	1.3	0.8
ClCH <sub>2</sub> CH <sub>2</sub> COO <sup>-</sup>	3.93	4.40	1.77 × 10 <sup>-2</sup>	7.3 × 10 <sup>-3</sup>	2.42	1.5
CH <sub>3</sub> COO <sup>-</sup>	4.65	5.17	3.55 × 10 <sup>-2</sup>	1.48 × 10 <sup>-2</sup>	2.40	1.7
(CH <sub>3</sub> ) <sub>2</sub> AsO <sub>2</sub> <sup>-</sup>	6.16	6.68	6.95 × 10 <sup>-1</sup>	1.92 × 10 <sup>-1</sup>	3.62	2.5

<sup>a</sup> Calculated from k<sub>B</sub><sup>H</sup>/k<sub>B</sub><sup>D</sup> by using eq 8 as described under Results. <sup>b</sup> Ballinger, P.; Long, F. A. *J. Am. Chem. Soc.* **1959**, *81*, 1050; **1960**, *82*, 795. <sup>c</sup> The Brønsted slopes were calculated for the data in H<sub>2</sub>O and are statistically corrected as described in ref 1a.

240 nm, or at 250 nm in methoxyacetic acid buffers, using a Hitachi U-2000 spectrophotometer. The absorbance of the buffer solution was initialized at zero, and data collection was started immediately upon injection of the hemiacetals into the buffer solution. Biphasic plots of absorbance against time were observed for all hemiacetals except for the acetaldehyde ethyl hemiacetal. The fast phase, τ<sub>1</sub>, is due to trapping of free acetaldehyde that is initially present upon mixing, and the slower phase, τ<sub>2</sub>, is due to the breakdown of the hemiacetal. The two kinetic processes were widely separated except for the acetaldehyde propargyl hemiacetal (τ<sub>1</sub>/τ<sub>2</sub> < 20).

Plots of absorbance against time were fit to eq 2<sup>29</sup> by a nonlinear least-squares fitting routine based on the Marquardt algorithm.<sup>30</sup> In eq 2 A<sub>i</sub> is the absorbance at time *t*, ΔA<sub>1</sub> and ΔA<sub>2</sub> refer to the fractional

$$A_i = A_\infty - \Delta A_1 e^{-t/\tau_1} - \Delta A_2 e^{-t/\tau_2} \quad (2)$$

amplitudes of the fast and slow phases, respectively, A<sub>∞</sub> is the final absorbance reading, and τ<sub>1</sub> and τ<sub>2</sub> refer to the relaxation times for the fast and slow phases, respectively. For ethanol hemiacetals, ΔA<sub>1</sub> was set equal to zero. Data were collected over a time period > 3.5τ<sub>2</sub>. The differences between the observed and calculated values for A<sub>∞</sub> were found to vary randomly by less than ±0.002A.

All catalytic constants, Brønsted slopes, and interaction coefficients were calculated by the method of least squares. Brønsted slopes were statistically corrected as described by Bell.<sup>1a</sup> Isotope effects were calculated by propagating the errors in the second-order rate constants according to

$$(A \pm a)/(B \pm b) = A/B \pm [(A/B)^2((a/A)^2 + (b/B)^2)]^{1/2} \quad (3)$$

in which *A* and *B* are the rate constants and *a* and *b* are the standard deviations.

## Results

The breakdown of acetaldehyde hemiacetals is catalyzed by both general acids and general bases.<sup>12</sup> The mechanisms of catalysis are altogether different, and only the experimental results for the general-base catalysis will be described in this paper.

The observed kinetic data are consistent with

$$1/\tau_2 = k_B[B^-] + k_{LB}[BL] + k_0 \quad (4)$$

where k<sub>B</sub> and k<sub>LB</sub> are the second-order rate constants for general-base and general-acid catalysis, respectively, B<sup>-</sup> is the basic component of the buffer, BL is the acidic component of the buffer, and k<sub>0</sub> is defined by

$$k_0 = k_L[L^+] + (k_{OL}/K_w[L^+]) + k_w \quad (5)$$

(29) Bernasconi, C. F. *Relaxation Kinetics*; Academic Press: New York, 1976; pp 142-143.

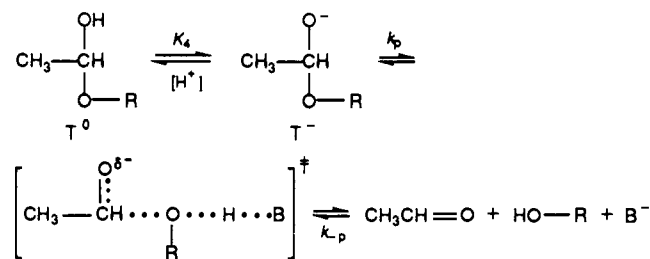
(30) Computer programs for the nonlinear least-squares fit to the data were kindly provided by Dr. Niel Stahl. The minimization of the residual deviations was performed by a program similar to that described by: Beech, G. *Fortran IV in Chemistry: An Introduction to Computer-Assisted Methods*; Wiley: New York, 1975; pp 41-47.

**Table II.** Buffer-Independent Rate Constants for the Breakdown of Acetaldehyde Hemiacetals CH<sub>3</sub>CH(OL)OR in Water and Deuterium Oxide

catalyst	k, M <sup>-1</sup> s <sup>-1</sup>		k <sup>H</sup> /k <sup>D</sup>	k <sub>p</sub> <sup>H</sup> /k <sub>p</sub> <sup>D</sup> <sup>a</sup>
	H <sub>2</sub> O	D <sub>2</sub> O		
	ROH = CH <sub>3</sub> CH <sub>2</sub> OH			
L <sub>2</sub> O	3 × 10 <sup>-3</sup> /55.5	1 × 10 <sup>-3</sup> /55.5	~3	—
OL <sup>-</sup>	1.66 × 10 <sup>4</sup>	2.90 × 10 <sup>4</sup>	0.57	0.8
	ROH = ClCH <sub>2</sub> CH <sub>2</sub> OH			
L <sub>2</sub> O	1 × 10 <sup>-3</sup> /55.5	0.5 × 10 <sup>-3</sup> /55.5	~2	—
OL <sup>-</sup>	8.03 × 10 <sup>5</sup>	9.73 × 10 <sup>5</sup>	0.82	1.2
	ROH = HC≡CCH <sub>2</sub> OH			
L <sub>2</sub> O	2.5 × 10 <sup>-3</sup> /55.5	0.4 × 10 <sup>-3</sup> /55.5	~6	—
OL <sup>-</sup>	4.91 × 10 <sup>6</sup>	7.28 × 10 <sup>6</sup>	0.67	1.0

<sup>a</sup> Isotope effect for decomposition of the tetrahedral intermediate T<sup>-</sup> in Scheme 1 "catalyzed" by water.

## Scheme I



in which K<sub>w</sub> is the ion product of water or deuterium oxide.

Figure 1 shows plots of 1/τ<sub>2</sub> against total buffer concentration at different fractions of free base for the breakdown of acetaldehyde propargyl hemiacetals catalyzed by acetic acid in water and deuterium oxide. The inset in the figure is a plot of the slopes vs f<sub>B</sub>, the fraction of the buffer in the basic form. Values of the second-order rate constants, k<sub>B</sub>, for general-base catalysis were obtained from the intercept of these plots at f<sub>B</sub> = 1 and are summarized in Table I along with the Brønsted coefficients in water calculated as described under Experimental Section.

The buffer-independent rate constants k<sub>0</sub> were obtained from the intercepts of the plots in Figure 1 and were fitted to eq 5 by a nonlinear least-squares fitting routine. Standard estimates of the errors in k<sub>L</sub> and k<sub>OL</sub> were less than ±5% and ±10%, respectively. The values for k<sub>w</sub> were uncertain by ±50%. The catalytic coefficients k<sub>OL</sub> and k<sub>w</sub> for the solvent-catalyzed breakdown of acetaldehyde hemiacetals are summarized in Table II. Values of k<sub>B</sub>, k<sub>LB</sub>, and k<sub>0</sub> for the breakdown of acetaldehyde hemiacetals with ethanol, chloroethanol, and propargyl alcohol

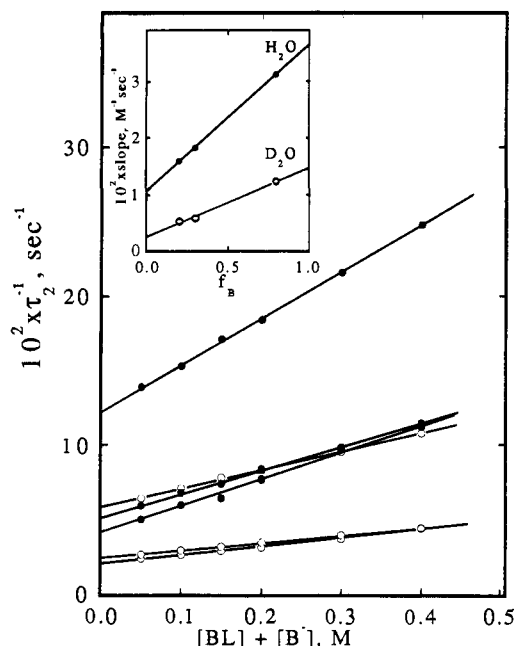


**Figure 1.** Dependence of  $1/\tau_2$  on the concentration of acetic acid in  $\text{H}_2\text{O}$  (●) and  $\text{D}_2\text{O}$  (○) for the breakdown of the propargyl hemiacetals of acetaldehyde. (Inset) Plots of the slopes vs the fractional amount of acetate ion,  $f_B$ . Values of the general-base catalytic coefficient,  $k_B$ , are obtained from the intercepts at  $f_B = 1.0$ .

leaving groups in water and deuterium oxide are summarized in supplementary Tables S1–S3.<sup>31</sup> The observed catalytic data for acetaldehyde ethyl hemiacetal show good agreement with previously reported second-order rate constants in  $\text{H}_2\text{O}$ .<sup>12,32</sup>

The observed general-base catalysis represents specific base general-acid catalysis as outlined in Scheme I. In Scheme I, an initial fast equilibrium ionization of the hemiacetal,  $\text{T}^0$ , to form the hemiacetal anion  $\text{T}^-$  is followed by a slow proton-transfer step that involves concerted leaving group expulsion that is stabilized by proton donation to the leaving group oxygen. This step is the microscopic reverse of eq 1.<sup>12</sup> The acid dissociation constant of the acetaldehyde hemiacetal,  $\text{T}^0$ , to form the hemiacetal anion,  $\text{T}^-$ , is defined by  $K_4$ .<sup>33</sup> The rate constant  $k_p$  for proton transfer to the leaving group oxygen can be described by

$$k_p = k_p^{\text{L}^2\text{O}} + k_p^{\text{L}}[\text{L}^+] + k_p^{\text{BL}}[\text{BL}] \quad (6)$$

The observed general-base catalytic coefficient  $k_B$  is related to the second-order rate constant  $k_p^{\text{BL}}$  according to

$$k_B[\text{B}^-] = (K_4/[\text{L}^+])k_p^{\text{BL}}[\text{BL}] = (K_4/K_a^{\text{BL}})k_p^{\text{BL}}[\text{B}^-] \quad (7)$$

where  $K_a^{\text{BL}}$  is the acid dissociation constant of the catalyst.

**Solvent Isotope Effects: General-Base Catalysis.** Solvent isotope effects for general-base catalysis of the breakdown of acetaldehyde hemiacetals,  $k_B^{\text{H}}/k_B^{\text{D}}$ , are summarized in Table I and have errors of <10% calculated as described under Experimental Section. The solvent deuterium isotope effect includes both the solvent isotope effect on the rate constant for proton transfer to the leaving group,  $k_p^{\text{BL}}$ , and the equilibrium isotope effects on the ionization constants of the hemiacetal,  $K_4$ , and the buffer,  $K_a^{\text{BL}}$ . The isotope effects for breakdown of the hemiacetal anion catalyzed by buffer acids,  $k_p^{\text{BH}}/k_p^{\text{BD}}$ , were calculated from eq 8 by assuming that the solvent

$$k_p^{\text{BH}}/k_p^{\text{BD}} = k_B^{\text{H}}K_a^{\text{BH}}K_4^{\text{D}}/k_B^{\text{D}}K_a^{\text{BD}}K_4^{\text{H}} \quad (8)$$

isotope effect on the ionization of acetaldehyde hemiacetals  $\Delta pK_4 = pK_4^{\text{D}} - pK_4^{\text{H}} = 0.67$  is the same as the solvent isotope effect on the ionization of aliphatic alcohols of  $pK = 12$ – $14$ .<sup>24,34</sup> A similar estimate<sup>17</sup> is obtained from the equation proposed by Bell,<sup>1a</sup>  $\Delta pK_4$

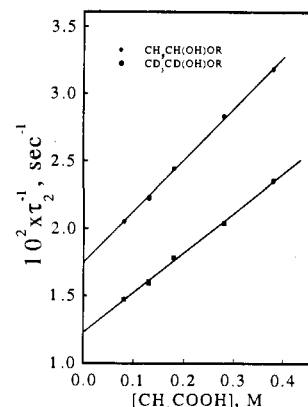


**Figure 2.** Dependence of  $1/\tau_2$  on the concentration of acetic acid ( $f_B = 0.85$ ) for the breakdown of the propargyl hemiacetals of acetaldehyde (●) and acetaldehyde- $d_4$  (■) in  $\text{H}_2\text{O}$ . The secondary  $\alpha,\beta$ -deuterium isotope effect on the second-order rate constant  $k_B$  is obtained from the ratio of slopes.

**Table III.** Secondary  $\alpha,\beta$ -Deuterium Isotope Effects for Decomposition of Acetaldehyde- $d_4$  Hemiacetals  $\text{CL}_2\text{CL}(\text{OH})\text{OR}^a$

fractional % base, $f_B$	$10^2 k_B, \text{M}^{-1} \text{s}^{-1}$		$k_B^{\alpha\text{BH}}/k_B^{\alpha\text{BD}}$		$\rho_n^b$
	L = H	L = D			
ROH = $\text{CH}_3\text{CH}_2\text{OH}$					
0.85	2.32	1.86	$1.25 \pm 0.038$	$1.21 \pm 0.021^c$	0.65
0.93	2.56	2.13	$1.20 \pm 0.021$		
ROH = $\text{HC}\equiv\text{CCH}_2\text{OH}$					
0.81	3.15	2.46	$1.28 \pm 0.068$		
0.85	3.19	2.47	$1.29 \pm 0.086$	$1.30 \pm 0.018^c$	0.48
0.91	3.33	2.52	$1.32 \pm 0.045$		

<sup>a</sup> Determined in acetic acid buffers in  $\text{H}_2\text{O}$  at 25 °C, 1.0 M (KCl).

<sup>b</sup> Fractional amount of change in the C–O bond order in the reverse, addition direction calculated from  $\rho_n = 1 - i$  using eq 9 as described under Results. <sup>c</sup> Calculated from the weighted mean of the secondary  $\alpha,\beta$ -deuterium isotope effects as described in ref 11.

$= 0.017pK_4 + 0.44$ , using the estimated values of  $pK_4 = 13.9$  for the acetaldehyde ethyl hemiacetal<sup>12</sup> and  $pK_4 = 13.4$  for ionization of acetaldehyde propargyl hemiacetal.<sup>33</sup> Values of  $k_p^{\text{BH}}/k_p^{\text{BD}}$  are summarized in Table I.

**Secondary  $\alpha,\beta$ -Deuterium Isotope Effects.** Figure 2 shows typical determinations of the second-order rate constants  $k_B$  for breakdown of acetaldehyde and acetaldehyde- $d_4$  hemiacetals catalyzed by acetic acid buffers according to eq 4. In these experiments, the ratio of the base to acid components of the buffers was chosen to give >88% general-base catalysis and the slopes in Figure 2 were used directly to calculate  $k_B$  as summarized in Table III. The secondary C–L isotope effects  $k_B^{\alpha\text{BH}}/k_B^{\alpha\text{BD}}$  are summarized in Table III for the propargyl and ethyl acetaldehyde hemiacetals.

An estimate of the relative change,  $i$ , in the bond order about the central carbon atom in going from the hemiacetal anion  $\text{T}^-$  to the transition state shown in Scheme I can be made from

$$k_p^{\alpha\text{BH}}/k_p^{\alpha\text{BD}} = (K^{\alpha\text{BH}}/K^{\alpha\text{BD}})i \quad (9)$$

where  $K^{\alpha\text{BH}}/K^{\alpha\text{BD}}$  is the equilibrium  $\alpha,\beta$ -deuterium isotope effect on  $k_p^{\text{BH}}$  and  $i$  varies from 0 to 1.<sup>11,36,37</sup>

(33) To facilitate comparison with the data of Sørensen and Jencks,<sup>12</sup> the equilibrium constants  $K_4$  in Scheme I and  $K_3$  in eq 10 are defined as in ref 12. The method for derivation of these equilibrium constants is described in detail by Funderburk et al.<sup>10</sup>

(34) The fractionation factors  $\phi_{\text{ROL}} = 1.25$  for the hydroxyl proton of hemiacetals determined by  $^1\text{H}$  NMR spectroscopy (Mata-Segreda, J. F.; Wint, S.; Schowen, R. L. *J. Am. Chem. Soc.* **1974**, *96*, 5604) are apparently in error.<sup>35</sup>

(35) Bone, R. L.; Wolfenden, R. *J. Am. Chem. Soc.* **1985**, *107*, 4772.

(36) Hogg, J. L.; Rodgers, J.; Kovach, I.; Schowen, R. L. *J. Am. Chem. Soc.* **1980**, *102*, 79.

(37) Gajewski, J. J. In *Isotopes in Organic Chemistry*; Buncl, E., Lee, C. C., Eds.; Elsevier: Amsterdam, 1987; Vol. 7, pp 115–176.

(31) See note concerning supplementary material at the end of the paper.

(32) Chiang, Y.; Kresge, A. J. *J. Org. Chem.* **1985**, *50*, 5038.

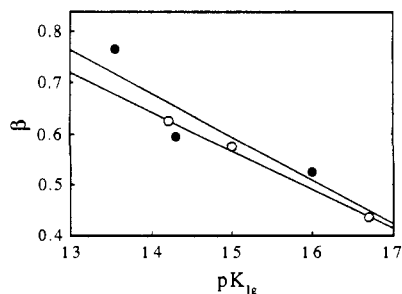


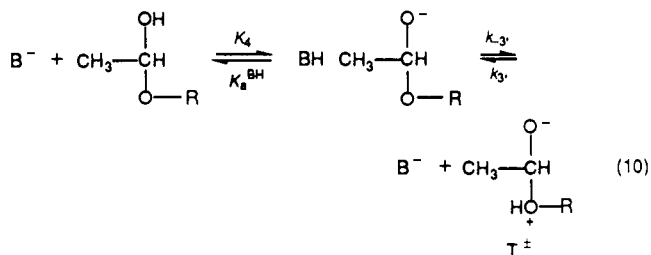
**Figure 3.** Dependence of the Brønsted  $\beta$  coefficient on the  $pK$  of the leaving group alcohol for general-base catalysis of the breakdown of acetaldehyde hemiacetals in  $H_2O$  (●) and in  $D_2O$  (○). The  $pK$  of the alcohols in  $D_2O$  were calculated from the estimated solvent isotope effect:<sup>17a</sup>  $\Delta pK = 0.017pK_{lg} + 0.44$  using literature values for the  $pK_a$  of the leaving group alcohols: Ballinger, P.; Long, F. A. *J. Am. Chem. Soc.* **1959**, *81*, 1050; Ballinger, P.; Long, F. A. *J. Am. Chem. Soc.* **1960**, *82*, 795.

The value of  $K^{\alpha\beta H}/K^{\alpha\beta D} = 1.60/1.04$  was taken as the product of the inverse equilibrium isotope effects for the nucleophilic addition of hydroxide ion to acetaldehyde,  $K^{\alpha H}/K^{\alpha D} = 1/0.72$  and  $K^{\beta H}/K^{\beta D} = 1/0.87$ ,<sup>36</sup> divided by the equilibrium isotope effect  $K_4^{\alpha H}/K_4^{\alpha D} = 1.04$  for ionization of the hemiacetal anion,  $K_4$  in Scheme I.<sup>38</sup> The latter correction is assumed to be the same as the equilibrium isotope effects on the dissociation constants of protonated amines.<sup>40</sup> The values of  $i$  are related to  $\rho_n$ , the normalized measure of the amount of C–OR bond formation in the reverse direction by  $i = 1 - \rho_n$ .<sup>11</sup> Table III summarizes values of  $\rho_n$ .

## Discussion

**General-Base Catalysis: Structure–Reactivity Behavior.** Table I summarizes values of the Brønsted  $\beta$  coefficients for catalysis by substituted acetate and cacodylate ions for breakdown of acetaldehyde hemiacetals with ethanol, chloroethanol, and propargyl alcohol leaving groups in water. The observed Brønsted coefficients  $\beta = 0.48$ – $0.72$  for general-base catalysis correspond to  $\alpha$  values of  $1 - \beta = 0.52$ – $0.38$  for general-acid catalysis of the breakdown of the hemiacetal anion,  $T^\ddagger$ , as illustrated in Scheme I. The Brønsted coefficients are consistent with concerted breakdown of the hemiacetal anion with a transition state involving partial C–O bond cleavage that is stabilized by proton transfer or hydrogen bonding to the leaving group oxygen.

Concerted cleavage of the hemiacetal anion is expected because the estimated second-order rate constant  $k_B \approx 10^{-6} M^{-1} s^{-1}$  for a stepwise mechanism involving rate-determining formation of the tetrahedral intermediate  $T^\ddagger$  as shown in eq 10 is some 2 orders



of magnitude *smaller* than the observed second-order rate constant  $k_B = 6.6 \times 10^{-3} M^{-1} s^{-1}$  for the breakdown of the propargyl alcohol hemiacetal catalyzed by methoxyacetate ion (Table I). The estimated second-order rate constant for rate-determining formation of  $T^\ddagger$  from the hemiacetal shown in eq 10 can be calculated from the observed rate constants and estimated ionization constants.

(38) The  $\beta$ -D equilibrium isotope effect on the ionization constant  $K_4$  is assumed to be unity on the basis of the equilibrium isotope effect  $K_4^{\alpha H}/K_4^{\alpha D} = 1.01$  for the ionization of acetic acid.<sup>3b</sup>

(39) Paabo, M.; Bates, R. G.; Robinson, R. A. *J. Phys. Chem.* **1966**, *70*, 540.

(40) Northcott, D.; Robertson, R. E. *J. Phys. Chem.* **1969**, *73*, 1559.

According to eq 10,  $k_B$  is given by  $k_B = k_{-3}K_4/K_a^{BH} = k_3K_4/K_3 \approx (10^{10} M^{-1} s^{-1})10^{-13.9}/10^2 \approx 10^{-6} M^{-1} s^{-1}$ ;  $k_3$ ; for the deprotonation of  $T^\ddagger$  by acetate ion in the reverse direction is assumed to be diffusion controlled,<sup>41</sup> and the acidity constant for ionization of the protonated ether  $T^\ddagger$  is estimated to be  $K_3 \approx 10^2$ .<sup>33</sup>

Figure 3 shows that there is a linear correlation between the Brønsted  $\beta$  coefficient and the  $pK$  of the leaving alcohol for the breakdown of acetaldehyde hemiacetals catalyzed by substituted acetate ions and cacodylate ion in  $H_2O$  and  $D_2O$ . The increase in the Brønsted  $\beta$  coefficient with a decrease in the  $pK$  of the leaving group alcohol can be described by the interaction coefficients  $p_{xy} = \partial\beta/\partial pK_{lg} = 0.090$  in  $H_2O$  and  $p_{xy} = 0.078$  in  $D_2O$  that describe the slopes of the lines in Figure 3. These interaction coefficients do not differ significantly from  $p_{xy} = 0.07$  determined by Sørensen and Jencks<sup>12</sup> with a more extensive set of leaving group alcohols in water.

**Secondary  $\alpha,\beta$ -Deuterium Isotope Effects.** Table III shows that there is an increase in the secondary  $\alpha,\beta$ -deuterium isotope effect as the  $pK$  of the leaving group alcohol is decreased for the breakdown of acetaldehyde hemiacetals catalyzed by acetate ion. The secondary  $\alpha$ - and  $\beta$ -deuterium isotope effects arise from changes in the vibrational frequencies of the C–L bonds (L = H or D) between reactant and transition states. These two isotope effects have fundamentally different origins. The  $\alpha$ -deuterium isotope effect is expected to be normal ( $k^{\alpha H} > k^{\alpha D}$ ), due largely to the decrease in the bending frequency of the  $\alpha$ -C–L bond to the central carbon that reflects the change in hybridization from  $sp^3$  to  $sp^2$ -like in the transition state.<sup>36,37</sup> The  $\beta$ -deuterium isotope effect originates from an increase in hyperconjugation of the three  $\beta$ -C–L bonds with the newly forming carbon–oxygen double bond that “loosens” the  $\beta$ -C–L bonds and gives rise to a normal kinetic isotope effect.<sup>37,42</sup>

The changes in hybridization about the central carbon atom that influence the magnitude of the secondary deuterium isotope effects are assumed to reflect the changes in C–O bond order between the central carbon and the developing carbonyl and leaving group oxygens. This assumption requires that the rule of the geometric mean<sup>43</sup> hold for these reactions, and force constants vary smoothly between the limiting force constants for reactants and products.<sup>45</sup> If these assumptions are correct, the changes in the  $\alpha,\beta$ -deuterium isotope effect with structure can be interpreted according to eq 9 as changes in bond order about the central carbon atom.

Indirect support for these assumptions comes from secondary  $\alpha$ -D and  $\beta$ -D<sub>3</sub> isotope effects for the mechanistically similar hydrolysis of aryl formates and acetates that show good agreement between measures of transition-state structure calculated from  $\alpha$ -D and  $\beta$ -D<sub>3</sub> isotope effects by using equations analogous to eq 9.<sup>46–48</sup> Semiempirical calculations of secondary  $\alpha$ -D and  $\beta$ -D<sub>3</sub> isotope effects for the nucleophilic addition of hydroxide ion to acetaldehyde show a monotonic change in the secondary isotope effects with changes in transition-state bond orders, although the assumption of linear changes in force constants with changes in bond order is inherent in the calculations.<sup>36</sup>

We conclude that the secondary  $\alpha,\beta$ -deuterium isotope effects reflect changes in bond order about the central carbon and show that heavy-atom motion is part of the reaction coordinate. If there is a monotonic change in the secondary isotope effects with changes in C–O bond order between the central carbon atom and the

(41) Eigen, M. *Angew. Chem., Int. Ed. Engl.* **1964**, *3*, 1.

(42) Shiner, V. J., Jr.; Cross, S. *J. Am. Chem. Soc.* **1957**, *79*, 3599.

(43) The rule of the geometric mean states that the isotope effect for the  $\alpha,\beta$ -deuterium-labeled substrates,  $k^{\alpha\beta H}/k^{\alpha\beta D}$ , is given by the product of the  $\alpha$ -deuterium,  $k^{\alpha H}/k^{\alpha D}$ , and  $\beta$ -deuterium,  $k^{\beta H}/k^{\beta D}$ , effects.<sup>44</sup>

(44) Bigeleisen, J. *J. Chem. Phys.* **1955**, *23*, 2264.

(45) Burton, G. W.; Sims, L. B.; McLennan, D. J. *J. Chem. Soc., Perkin Trans. 2* **1977**, 1763.

(46) do Amaral, L.; Bastos, M. P.; Bull, H. C.; Ortiz, J. J.; Cordes, E. H. *J. Am. Chem. Soc.* **1979**, *101*, 169.

(47) Kovach, I. M.; Elrod, J. P.; Schowen, R. L. *J. Am. Chem. Soc.* **1980**, *102*, 7530.

(48) Stein, R. L.; Elrod, J. P.; Schowen, R. L. *J. Am. Chem. Soc.* **1983**, *105*, 2446.

leaving group oxygen, the C–L isotope effects suggest that the C–O leaving group bond has been approximately 50% cleaved as measured by  $i = 1 - \rho_n$  (Table III).

The change in the secondary  $\alpha,\beta$ -deuterium isotope effect with changes in the pK of the leaving group can be described quantitatively by the interaction coefficient  $p_{yy}$  according to

$$p_{yy} = \partial \rho_n / -\partial pK_{lg} \quad (11)$$

where  $\rho_n$  is a measure of the amount of bond rehybridization at the carbonyl carbon as described under Results. A negative value of  $p_{yy} = -0.069$  is derived from the data in Table III. A less negative value of the coefficient  $p_{yy} = -0.05$  was determined from (a) increases in the secondary  $\alpha$ -deuterium isotope effects with decreasing pK of the leaving group alcohol for the general-base-catalyzed breakdown of formaldehyde- $d_2$  hemiacetals<sup>11</sup> and (b) increases in the rate constant ratios with decreasing pK of the leaving group alcohol for the breakdown of acetaldehyde and formaldehyde hemiacetals.<sup>12</sup>

**Solvent Isotope Effects.** Table I shows that the solvent isotope effects  $k_p^{\text{BH}}/k_p^{\text{BD}}$  for general-acid-catalyzed cleavage of the hemiacetal anion are small and essentially independent of the pK of the leaving group alcohol. The isotope effects correspond to isotopic fractionation factors<sup>49</sup>  $\phi^T = \phi_{\text{BL}} k_p^{\text{BD}}/k_p^{\text{BH}} = 0.40$ – $1.2$ .

Mechanistic deductions from solvent isotope effects for proton transfers between electronegative atoms are sometimes hampered by the uncertainty in the corrections for small secondary equilibrium isotope effects.<sup>7,23</sup> However, the isotope effects that we assign to the catalytically active proton are unlikely to represent secondary isotope effects since the correction for these effects is small. The largest uncertainty associated with the isotope effect for the transferred proton is due to the uncertainty in the estimate for the equilibrium solvent isotope effect for the ionization of the hemiacetal  $K_4^{\text{H}}/K_4^{\text{D}}$ . Although this equilibrium isotope effect is an estimated value, it is unlikely to vary significantly with changes in the pK of the leaving group alcohol. Comparison of the relative isotope effects with changes in the pK of the catalyst or the leaving group alcohol have less uncertainty. We conclude that the solvent isotope effects  $k_p^{\text{BH}}/k_p^{\text{BD}} = 0.8$ – $2.5$  summarized in Table I are primary isotope effects due to the catalytically active proton shown in the transition state of Scheme 1.

Although there is a small tendency for the solvent isotope effect  $k_p^{\text{BH}}/k_p^{\text{BD}}$  to decrease for the stronger acid catalysts for a given hemiacetal, the absence of a significant isotope effect maximum provides further evidence for a concerted reaction mechanism. A maximum isotope effect  $k_p^{\text{BH}}/k_p^{\text{BD}} = 3$ – $5$  would be expected for the stepwise mechanism that involves rate-determining proton transfer to form the tetrahedral intermediate  $\text{T}^\ddagger$  as shown in eq 10 when  $\Delta pK = pK_{\text{a}}^{\text{BL}} - pK_3 = 0$ . According to the simple three-center model for proton transfer proposed by Westheimer<sup>52</sup> and Melander<sup>53</sup> the zero-point energy of the B–H bond may be retained in the transition state in the symmetric vibration orthogonal to the reaction coordinate. The contribution of this symmetric stretching vibration to the zero-point energy of the transition state will be smallest for thermoneutral proton transfers which are expected to show the maximum isotope effect. Estimates<sup>33</sup> of the pK of the protonated ether intermediate  $\text{T}^\ddagger$  shown in eq 10 range from  $pK_3 = 0.4$  to  $-2$ , so the isotope effect should increase for the stronger acid catalysts as the proton transfer becomes more thermodynamically favorable. However, the data

in Table I show that the isotope effect  $k_p^{\text{BH}}/k_p^{\text{BD}}$  approaches  $1.0 \pm 0.2$  for the stronger acid catalysts that correspond to  $\Delta pK \sim 3$ – $5$ .

There is evidence for a maximum in the solvent isotope effects near  $\Delta pK \sim 0$  for proton transfer between electronegative atoms involving the stepwise trapping mechanisms of the transamination of hydroxylamine and benzhydrylidenedimethylammonium ion catalyzed by general bases,<sup>54</sup> the general-acid-catalyzed addition of methoxyamine to *p*-methoxybenzaldehyde<sup>55</sup> and phenyl acetate,<sup>56</sup> and the general-base-catalyzed aminolysis of methyl formate by aniline.<sup>57</sup> Such isotope effect maxima require a significant difference in curvature in the Brønsted plots for acid or base catalysis in  $\text{H}_2\text{O}$  and  $\text{D}_2\text{O}$  which is not observed in the reactions of hemiacetal anions (data not shown). The isotope effect maxima have generally been interpreted in terms of the three-step Eigen mechanism for proton transfer between electronegative atoms,<sup>41</sup> although so-called Melander–Westheimer effect may also be consistent with the experimental data in some cases.<sup>56</sup>

There is evidence for small solvent isotope effects that are independent of the pK of the catalyst for concerted general-base-catalyzed addition of water<sup>26,54</sup> and amines<sup>58</sup> to stable electrophiles. The addition of pyrazole to substituted phenyl acetates<sup>58</sup> is catalyzed by general bases and shows small solvent isotope effects  $k_{\text{B}}^{\text{H}}/k_{\text{B}}^{\text{D}} = 1.8 \pm 0.2$ .<sup>59</sup> The addition of water to benzhydrylidenedimethylammonium ion<sup>53</sup> and to 1,3-dichloroacetone<sup>26</sup> catalyzed by substituted acetate ions shows small isotope effects  $k_{\text{B}}^{\text{H}}/k_{\text{B}}^{\text{D}} = 1.9 \pm 0.2$  and  $k_{\text{B}}^{\text{H}}/k_{\text{B}}^{\text{D}} = 2.8 \pm 0.2$ , respectively. It is difficult to interpret these isotope effects because of the uncertainty in the secondary solvent isotope effects due to the second proton of the attacking water molecule. However, the absence of any significant change in the solvent isotope effects with changes in the pK of the catalyst is consistent with our observations for the microscopic reverse decomposition of hemiacetal anions. Taken together, these data suggest that the absence of a significant change in the solvent isotope effect for proton transfer in multibond reactions is consistent with a reaction coordinate that is dominated by heavy-atom motion that increases the effective mass of the transferred proton and lowers the isotope effect.<sup>13</sup>

**Solvent-Catalyzed Pathways.** Table II summarizes the second-order rate coefficients and isotope effects for the solvent species  $\text{OL}^-$  and  $\text{L}_2\text{O}$ . The solvent isotope effects for protonation of  $\text{T}^-$  by  $\text{L}_2\text{O}$ ,  $k_p^{\text{H}_2\text{O}}/k_p^{\text{D}_2\text{O}} = 1 \pm 0.2$ , are derived from the lyoxide ion catalytic coefficients,  $k_{\text{OL}} = k_p^{\text{L}_2\text{O}} K_{\text{a}}/K_{\text{a}}^{\text{L}_2\text{O}}$ . They are consistent with stepwise expulsion from the hemiacetal anion of the alkoxide ion that is hydrogen bonded to water, as previously suggested on the basis of the large values of  $\beta_{\text{lg}} = -0.7$  to  $-1.1$  for hydroxide ion catalysis.<sup>12</sup>

**Concerted Breakdown of the Hemiacetal Anion.** The change in the secondary  $\alpha,\beta$ -deuterium isotope effects and Brønsted coefficients with reactant structure are consistent with a coupling between the amount of proton transfer from the catalyst with the change in bond order or charge on the central oxygen in a concerted transition state for breakdown of the hemiacetal anion. These changes can be described by the More O'Ferrall–Jencks diagram shown in Figure 4.<sup>3</sup> The  $x$  axis is defined by the Brønsted  $\beta$  coefficient representing proton transfer and the  $y$  axis is  $\rho_n$  for C–O bond cleavage/formation. The values of  $\rho_n$  and  $\beta$  define the range of movement of the transition state with changes in substituent. The diagram provides a convenient way to visualize changes in transition-state structure in terms of experimentally

(49) Isotopic fractionation factors are an alternative way to express observed solvent isotope effects in terms of ground-state and transition-state effects for the individual hydrogenic sites.<sup>14</sup> This analysis neglects medium effects and assumes that (a) the proton-transfer step as shown in Scheme 1 is direct and (b)  $\phi_{\text{BL}} = 1.00$  for substituted acetic acids and cacodylic acid.<sup>17</sup> This latter assumption is undoubtedly an oversimplification since the hydrogen bond strength of  $\text{RCOOH}\cdot\text{OH}_2$  depends upon the pK of  $\text{RCOOH}$ .<sup>50</sup> However, the fractionation factor  $\phi_{\text{BL}} = 0.87$  for maleic and succinic acid that have strong intermolecular hydrogen bonds<sup>51</sup> suggests that the fractionation factors for substituted acetic acids should not vary substantially with pK.

(50) Murray, C. J.; Jencks, W. P. *J. Am. Chem. Soc.* **1988**, *110*, 7561.

(51) Jarret, R. M.; Saunders, M. J. *J. Am. Chem. Soc.* **1985**, *107*, 2648.

(52) Westheimer, F. H. *Chem. Rev.* **1961**, *61*, 265.

(53) Reference 1d, pp 130–140.

(54) Fischer, H.; DeCandis, F. X.; Ogden, S. D.; Jencks, W. P. *J. Am. Chem. Soc.* **1980**, *102*, 1340.

(55) Bergman, N.-Å.; Chiang, Y.; Kresge, A. J. *J. Am. Chem. Soc.* **1978**, *100*, 5954.

(56) Cox, M. M.; Jencks, W. P. *J. Am. Chem. Soc.* **1981**, *103*, 572.

(57) Yang, C. C.; Jencks, W. P. *J. Am. Chem. Soc.* **1988**, *110*, 2972.

(58) Fishbein, J. C.; Baum, H.; Cox, M. M.; Jencks, W. P. *J. Am. Chem. Soc.* **1987**, *109*, 5790.

(59) However, somewhat surprisingly the large change in the Brønsted  $\beta$  coefficient with changes in catalyst pK that can be described by  $p_x = \partial\beta/\partial pK = 0.1$  is consistent with a reaction coordinate that consists almost entirely of proton motion.<sup>58</sup>

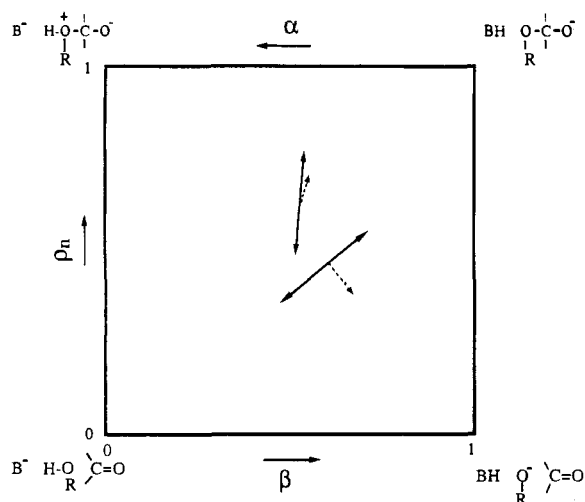


**Figure 4.** More O'Ferrall-Jencks diagram that is defined by the structure-reactivity parameters. The  $x$  axis refers to proton transfer as defined by  $\beta$ , and the  $y$  axis refers to C-O bond breaking/formation, as defined by the normalized  $\rho$  value calculated from the secondary  $\alpha, \beta$ -deuterium isotope effects as described under Results. The solid lines describe the relative contributions of changes in proton transfer and heavy-atom reorganization to the reaction coordinate that corresponds to the decomposition mode of the transition state to reactants or products. The dashed lines show the effect of introducing an electron-withdrawing group on the alcohol on the position of the transition state for diagonal (proton transfer and heavy-atom reorganization coupled) and vertical (proton transfer and heavy-atom reorganization uncoupled; hydrogen bonding) reaction coordinates.

observed parameters such as isotope effects and structure-reactivity correlations.<sup>60</sup>

For example, for a diagonal reaction coordinate through the center of the diagram, a change to a more electron withdrawing group on the alcohol will destabilize the hypothetical protonated intermediate  $T^\ddagger$  in the upper left hand corner of the diagram and stabilize the alkoxide ion in the lower right. This will shift the transition state largely perpendicular to the reaction coordinate as illustrated by the dashed line in Figure 4.<sup>61</sup> This shift will result in an increase in the amount of proton transfer, as measured by  $\beta$  (Table I) and a decrease in the amount of C-O bond formation, as measured by  $\rho_n$  (Table III).

The observed changes in structure-reactivity coefficients are inconsistent with a reaction coordinate that involves predominantly heavy-atom motion with the proton in a potential well. This reaction coordinate would correspond to the largely vertical reaction coordinate shown in Figure 4. A more electron withdrawing group on the leaving alcohol would result in a shift in transition-state structure that is largely parallel (Hammond effect) to the reaction coordinate with an increase in the amount of C-O bond formation as measured by  $\rho_n$  and little or no change in the amount of proton transfer as measured by  $\beta$ .

#### Hydrogen-Bonded Transition States in Multibond Reactions.

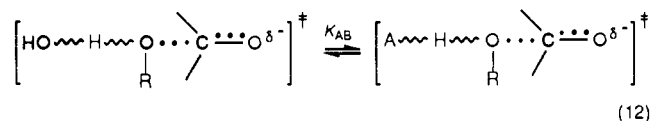
The structure-reactivity coefficients,  $\beta$  and  $i = 1 - \rho_n$ , estimates of second-order rate constant for stepwise breakdown of the hemiacetal anion, the small solvent isotope effects for the catalytically active proton, and the changes in the structure-reactivity coefficients with changes in the acidity of the leaving group alcohol, provide evidence for a concerted reaction mechanism for the breakdown of the hemiacetal anion ( $k_p$  step in Scheme I). In the reverse direction, this corresponds to general-base-catalyzed attack of alcohols on aldehydes as shown in eq 1. These results confirm the conclusion that the general-acid catalysis of the breakdown of the hemiacetal anions involves concerted leaving group expulsion

that is stabilized by proton donation to the leaving group in a coupled, concerted transition state.<sup>10-12</sup>

The results do not require a hydrogen-bonded proton in these simple reactions and suggest that hydrogen-bonding catalysis may not be required in mechanistically similar reactions such as the hydrolysis of acetals, ketals, and ortho esters catalyzed by general acids or ester or amide hydrolysis catalyzed by hydrolytic enzymes. The evidence in support of these conclusions can be summarized as follows:

(1) Changes in structure-reactivity relationships with catalyst and leaving group  $pK$  can be described by a diagonal reaction coordinate on structure-reactivity diagrams such as Figure 4.<sup>10-12</sup> Most notably, a negative value for the coefficient  $p_{yy'} = \partial \rho_n / -\partial pK_{lg}$  is consistent with a diagonal reaction coordinate with significant coupling between the amount of proton transfer and heavy-atom motion in the transition state. The changes are incompatible with a proton in a potential well where a positive value for the  $p_{yy'}$  coefficient is expected.<sup>11,62</sup>

(2) For hydrogen bonding between a catalyst AH and the leaving group alcohol to compete with the solvent in the transition state for the breakdown of hemiacetal anions (eq 12), there must



be a change in the strength of the hydrogen bond interaction described by  $K_{AB}$  with changes in the  $pK_{BH}$  of the transition state and changes in the  $pK_{AH}$  of the catalyst. These changes represent an electrostatic interaction between the catalyst and the leaving group oxygen in the transition state and should follow the relationship proposed by Hine:<sup>19</sup>

$$\tau = \frac{\partial^2 \log K_{AB}}{\partial \log K_{AH} \partial \log K_{BH}} \quad (13)$$

A value for the hydrogen bond interaction coefficient  $\tau \geq 0.028$  is required to account for the observed catalysis by a hydrogen-bonding mechanism.<sup>63</sup> This is substantially larger than values of  $\tau = 0.013$  for hydrogen bond interactions between stable molecules in water.<sup>64</sup>

The distance across the A-H-O hydrogen bond in the transition state of eq 12 might be compressed, relative to the ground state, such that there is little, if any, barrier for motion of the proton across the hydrogen bond.<sup>9,16</sup> This would be consistent with both an increase in the value of  $\tau$  and Hine's estimate of  $\tau = 0.054$  for a symmetrically hydrogen bonded proton with no barrier for motion of the proton that corresponds to the maximum value of  $\tau$  in water.<sup>19</sup> However, the concept of solvation catalysis, as originally described by Swain et al.,<sup>15</sup> requires that "transition-state OH bonds...be of intermediate character" between the reactant and product OH bonds. This assumption, implicit within the framework of transition-state theory, is based on the hypothesis of a quasi-equilibrium between ground states and transition states that suggests that electrostatic interactions of polar groups can be treated in a similar way for ground states and transition states.<sup>60</sup> It suggests that solvation catalysis as originally defined is in-

(62) There is evidence based on the positive  $p_{yy'}$  interaction coefficient for a hydrogen-bonded transition state in the general-base-catalyzed addition of alcohols to unstable carbocations: Ta-Shma, R.; Jencks, W. P. *J. Am. Chem. Soc.* **1986**, *108*, 8040.

(63) This estimate is based on a modified form of the Hine equation:<sup>64</sup>  $\tau = (\log K_{AB} + 2.04) / [(pK_{AH} - pK_{H_2O})(pK_{H_3O^+} - pK_{BH})]$ . The value of  $\tau$  was calculated by using the upper limit for the  $pK_{BH} = 16$  of the transition state assuming full negative charge buildup on the leaving group oxygen and a value of  $K_{AB}$  calculated from the ratio of rate constants  $(k_B/k_{OH})(K_a^{BH}/K_a^{H_2O}) = k_p^{BH}/(k_p^{H_2O} 55) = K_{AB} = 2.61 \times 10^3 \text{ M}^{-1}$  for breakdown of the anion of acetaldehyde ethyl hemiacetal catalyzed by acetic acid,  $pK_{AH} = 4.7$ . This represents a lower limit for the value of  $\tau$  because the  $pK_{BH}$  of the transition state will be smaller due to partial bonding between the central carbon and the leaving group oxygen in the transition state that decreases the amount of negative charge on the leaving group oxygen and lowers the  $pK_{BH}$ .

(64) Stahl, N.; Jencks, W. P. *J. Am. Chem. Soc.* **1986**, *108*, 4196.

(60) Jencks, W. P. *Bull. Soc. Chim. Fr.* **1988**, 218.

(61) Perpendicular, or "anti-Hammond", effects represent movement toward the more stable intermediate and parallel, or "Hammond", effects represent movement away from the more stable intermediate. The amount of the movements depend upon the magnitude and sign of the curvatures perpendicular and parallel to the reaction coordinate.<sup>3</sup>



consistent with compression of reacting groups across a hydrogen bond.

(3) The solvent kinetic isotope effects in the range  $k_p^{BH}/k_p^{BD} = 0.8-2.5$  for proton transfer to the leaving group oxygen in the breakdown of acetaldehyde hemiacetals anions are consistent with similar relative contributions of proton transfer and heavy-atom motion along the reaction coordinate that increases the effective mass of the transferred proton and decreases the isotope effect.<sup>13</sup> This effect can be modeled by using vibrational analysis calculations as described in detail in the following paper.

The results show that the small magnitude of solvent kinetic isotope effects in multibond reactions cannot, in and of themselves, be used as a criteria for solvation catalysis via hydrogen-bonded transition states. We suggest that the solvent isotope effects  $k_{H_2O}/k_{D_2O} = 1.6-4$  for ester and amide hydrolysis catalyzed by hydrolytic enzymes<sup>17</sup> can be interpreted within the framework of

a fully coupled, concerted mechanism without the requirement for compression of hydrogen-bonded groups on the enzyme.

**Acknowledgment.** This research was supported in part by grants from NIH (GM43251) and the donors of the Petroleum Research Fund, administered by the American Chemical Society.

**Registry No.** H<sub>3</sub>CCH(OH)OEt, 7518-70-9; H<sub>3</sub>CCH(OH)OCH<sub>2</sub>C<sub>2</sub>H<sub>5</sub>, 108743-22-2; H<sub>3</sub>CCH(OH)OCH<sub>2</sub>C≡CH, 2187-89-5; D<sub>2</sub>, 7782-39-0.

**Supplementary Material Available:** Tables S1-S3 summarizing second-order rate constants  $k_B$  and  $k_{LB}$  for general-base and general-acid catalysis and rate constants  $k_0$  for breakdown of acetaldehyde and acetaldehyde-*d*<sub>4</sub> hemiacetals in water and deuterium oxide (5 pages). Ordering information is given on any current masthead page.

## Characterization of Transition States by Isotopic Mapping and Structure-Reactivity Coefficients: Vibrational Analysis Calculations for the General-Base-Catalyzed Addition of Alcohols to Acetaldehyde

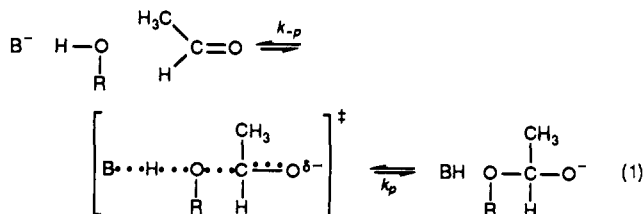
Christopher J. Murray\* and Timothy Webb

Contribution from the Department of Chemistry and Biochemistry, University of Arkansas, Fayetteville, Arkansas 72701. Received May 7, 1990

**Abstract:** General-base catalysis of the breakdown of acetaldehyde hemiacetals represents equilibrium ionization of the hemiacetal CH<sub>3</sub>CH(OH)OR to form the hemiacetal anion, CH<sub>3</sub>CH(O<sup>-</sup>)OR, followed by rate-determining general-acid catalysis of the cleavage of the hemiacetal anion to form acetaldehyde and ROH as described in the previous paper. Solvent deuterium isotope effects for the kinetically equivalent reverse reaction, general-base-catalyzed addition of alcohols ROH to acetaldehyde, have been modeled by using vibrational analysis calculations. Two independent weighting parameters that describe the bond orders for the catalyst O-H bond ( $W_{OH}$ ) and the C-O bond between the central carbon and oxygen atoms ( $W_{CO}$ ) were allowed to vary independently between 0 and 1 to generate isotopic maps as a function of transition-state structure. The effect of coupling of proton transfer to heavy-atom motion on the magnitude of the solvent kinetic isotope effect  $k_{H_2O}/k_{D_2O}$  was investigated by varying the relative ratios of several interaction force constants  $f_{ij}$  that couple two internal stretching coordinates. This process generates models of the reaction-coordinate motion for decomposition of the transition state to reactants and products. It is concluded that a reaction coordinate with essentially equal contributions of proton and heavy-atom motion is most consistent with the experimental isotope effects  $(k_p^B)_{H_2O}/(k_p^B)_{D_2O} = 1.7 \pm 0.5$  for general-base catalysis of the addition of alcohols to acetaldehyde.

### Introduction

The preceding paper<sup>1</sup> describes experimental evidence using kinetic isotope effects that confirms and extends evidence based on changes in structure-reactivity coefficients for a fully coupled, concerted reaction mechanism for the breakdown of acetaldehyde hemiacetals anions. In the reverse direction, this reaction corresponds to a class n reaction involving the general-base-catalyzed attack of alcohols on acetaldehyde.



(1) Colman, C. A.; Murray, C. J. *J. Am. Chem. Soc.* **1991**, previous paper in this issue.

In this paper we describe a method of characterizing the transition-state structure in eq 1 using model vibrational analysis calculations of the solvent isotope effects.<sup>2,3</sup> An important streamlining of the modeling process has been developed by Schowen and his co-workers,<sup>4-6</sup> who suggested that the properties

(2) For details on vibrational analysis calculations of isotope effects see: (a) Van Hook, W. A. In *Isotope Effects in Chemical Reactions*; Collins, C. J., Bowman, N. S., Eds.; Van Nostrand-Reinhold: Princeton, NJ, 1970; pp 1-89. (b) Melander, L.; Saunders, W. H., Jr. *Reaction Rates of Isotopic Molecules*; Wiley: New York, 1980. (c) Sims, L. B.; Lewis, D. E. In *Isotopes in Organic Chemistry*; Buncl, E., Lee, C. C., Eds.; Elsevier: New York, 1980; pp 161-259. (d) McClellan, D. J. In *Isotopes in Organic Chemistry*; Buncl, E., Lee, C. C., Eds.; Elsevier: New York, 1987; pp 393-480.

(3) Buddenbaum, W. E.; Shiner, V. J., Jr. In *Isotope Effects on Enzyme-Catalyzed Reactions*; Cleland, W. W., O'Leary, M. H., Northrop, D. B., Eds.; University Park Press: Baltimore, MD, 1977; pp 1-36.

(4) Hogg, J. L.; Rodgers, J.; Kovach, I.; Schowen, R. L. *J. Am. Chem. Soc.* **1980**, *102*, 79.

(5) Rodgers, J.; Femac, D. A.; Schowen, R. L. *J. Am. Chem. Soc.* **1982**, *104*, 3263.

(6) Huskey, W. P. Ph.D. Thesis, University of Kansas, 1985.